UC Berkeley
UC Berkeley Previously Published Works

Title
Protective Effect of Inflammasome Activation by Hydrogen Peroxide in a Mouse Model of Septic Shock

Permalink
https://escholarship.org/uc/item/2cf349rq

Journal
Critical Care Medicine, 45(2)

ISSN
0090-3493

Authors
Huet, Olivier
Pickering, Raelene J
Tikellis, Chris
et al.

Publication Date
2017-02-01

DOI
10.1097/ccm.0000000000002070

Peer reviewed

eScholarship.org Powered by the California Digital Library
University of California

Protective Effect of Inflammasome Activation by Hydrogen Peroxide in a Mouse Model of Septic Shock

Olivier Huet, MD, PhD[1,2,3]; Raelene J. Pickering, PhD[1]; Chris Tikellis, PhD[1]; Celine Latouche, PhD[1]; Fenella Long, PhD[1]; Bronwyn Kingwell, PhD[1]; Bryan Dickinson, PhD[5]; Chris J. Chang, PhD[5]; Seth Masters, PhD[4]; Fabienne Mackay, PhD[3]; Mark E. Cooper, MD, PhD[1]; Judy B. de Haan, PhD[1]

Objectives: To study the effect of a lack of antioxidant defenses during lethal pneumonia induced by *Klebsiella pneumonia*, compared to wild-type mice.

Setting: Laboratory experiments.

Subjects: C57Bl6 and glutathione peroxidase 1 knockout mice.

Intervention: Murine acute pneumonia model induced by *Klebsiella pneumonia*.

Measurements and Main Results: We show here that despite a lack of one of the major antioxidant defense enzymes, glutathione peroxidase 1 knockout mice are protected during lethal pneumonia induced by *Klebsiella pneumonia*, compared to wild-type mice. Furthermore, this protective effect was suppressed when antioxidant defenses were restored. Infected glutathione peroxidase 1 mice showed an early and significant, albeit transient, increase in the activity of the NOD-like receptor family, pyrin domain containing 3 inflammasome when compared with wild-type mice. The key role of the NOD-like receptor family, pyrin domain containing 3 inflammasome during acute pneumonia was confirmed in vivo when the protective effect was suppressed by treating glutathione peroxidase 1 mice with an interleukin-1 receptor antagonist. Additionally we report, in vitro, that increased concentrations of active caspase-1 and interleukin-1β are related to an increased concentration of hydrogen peroxide in bacterially infected glutathione peroxidase 1 macrophages and that restoring hydrogen peroxide antioxidant defenses suppressed this effect.

Conclusions: Our findings demonstrate that, contrary to current thinking, an early intervention targeting NOD-like receptor family, pyrin domain containing 3 inflammasome activity induces a timely and efficient activation of the innate immune response during acute infection. Our findings also demonstrate a role for hydrogen peroxide in the mechanisms tightly regulating NOD-like receptor family, pyrin domain containing 3 activation. (*Crit Care Med* 2017; 45:e184–e194)

Key Words: antioxidant defense; caspase-1; hydrogen peroxide; glutathione peroxidase; inflammasome; innate immune response; interleukin-1β; sepsis; septic shock

[1]Diabetes Complications, BakerIDI Heart and Diabetes Institute, Melbourne, VIC, Australia.

[2]Department of Anaesthesia and Intensive Care, CHRU La Cavale Blanche, Université de Bretagne Ouest, Brest, France.

[3]Australian and New Zealand Intensive Care Research Centre, School of Public Health and Preventive Medicine, Monash University, Melbourne, VIC, Australia.

[4]Inflammation Division, The Walter and Eliza Hall Institute, Parkville, VIC, Australia.

[5]Departments of Chemistry and Molecular and Cell Biology and the Howard Hughes Medical Institute, University of California, Berkeley, CA.

Drs. Huet and de Haan designed experiments, critically evaluated the results, and wrote the article. Drs. Huet, Pickering, Tikellis, Latouche, and Long performed experiments. Drs. Dickinson and Chang designed and synthesized the PF6-AM fluorescent probe. Drs. Kingwell, Masters, Mackay, and Cooper were involved in study design and article editing.

Supplemental digital content is available for this article. Direct URL citations appear in the printed text and are provided in the HTML and PDF versions of this article on the journal's website (http://journals.lww.com/ccmjournal).

Supported in part by the Victorian Government's Operational Infrastructure Support Program.

Dr. Huet was supported in part by an SFAR fellowship. Dr. Tikellis received support for this article research from the National Health and Medical Research, Canberra, Australia. Dr. Kingwell's institution received funding from the Victorian state government. Dr. Chang received support for this article research from the National Institutes of Health and Howard Hughes Medical Institute. The remaining authors have disclosed that they do not have any potential conflicts of interest.

For information regarding this article, E-mail: olivier.huet@chu-brest.fr

Copyright © 2017 by the Society of Critical Care Medicine and Wolters Kluwer Health, Inc. All Rights Reserved.

DOI: 10.1097/CCM.0000000000002070

A recent worldwide survey reported that 29.5% of patients admitted to ICU had sepsis at admission or during their ICU stay, with a mortality rate among those affected of 25.8% (1).

A prolonged and increased nonspecific systemic inflammatory response (2) and enhanced oxidative stress (3) have been considered to be contributors to severe sepsis. This rationale has been used to justify several large randomized clinical trials intended to blunt the inflammatory response, none of which have succeeded (4). These failures highlight our

Copyright © 2016 by the Society of Critical Care Medicine and Wolters Kluwer Health, Inc. All Rights Reserved.

limited knowledge of the mechanisms leading to severe sepsis, and current studies suggest that a more complex coexistence of pro- and anti-inflammatory responses is involved, with a specific temporal relationship (5–7). Recent clinical reports focusing on the early stages of infection stress the critical need for a strong and transient proinflammatory response to generate a better clinical outcome during acute infections (8, 9). Furthermore, it has been shown that the ratio of pro- to anti-inflammatory factors changes during disease progression, and this ratio seems to be key to the avoidance of septic shock (9).

The NOD-like receptor family, pyrin domain containing 3 (NLRP3) inflammasome controls the activation of two proinflammatory cytokines: interleukin (IL)-1β and IL-18. IL-1β, a key proinflammatory cytokine involved in the innate immune response, is synthesized as an inactive precursor that becomes activated after cleavage by caspase-1. When activated, both caspase-1 and IL-1β are secreted out of the cell, which is a hallmark feature of the activated inflammasome. The NLRP3 inflammasome plays a key role during infection, as recently shown for a bacterial model of septic shock where its inactivation induced higher mortality (10, 11).

Cellular mechanisms controlling the activation of the inflammasome are not fully understood (12). Recent evidence suggests a role for reactive oxygen species (ROS), but this remains to be fully delineated. It has been hypothesized that the NLRP3 inflammasome is a general sensor of cellular stress through its activation by ROS that have been generated in the proximity of the inflammasome (13–16). However, the specific ROS and the mechanism by which the NLRP3 inflammasome senses ROS are currently unclear and remain controversial.

Using an endotoxemic murine model, it has been reported that the absence of the cytosolic Cu/Zn isoform, superoxide dismutase (SOD)1, is followed by inactivation of the NLRP3 inflammasome in vitro and in vivo (16). The absence of SOD1 activity significantly increases the concentration of $O_2^{\cdot-}$ by suppressing its dismutation into hydrogen peroxide (H_2O_2). Indeed, oxidation of key inflammasome proteins mediated by $O_2^{\cdot-}$ was shown to prevent inflammasome activation (16). SOD1 was, therefore, hypothesized to play a key role in the activation of the NLRP3 inflammasome. However, a role for H_2O_2 cannot be ruled out given its rapid formation due to dismutation by SOD1. Given that H_2O_2 is involved in numerous cell-signaling pathways, we hypothesized that H_2O_2 may regulate the activation of the NLRP3 inflammasome. To directly test this hypothesis, we have used mice deficient in the ubiquitous cytoplasmic enzyme glutathione peroxidase 1 ($GPx1^{-/-}$) in a model of acute pneumonia induced by live bacteria, *Klebsiella pneumoniae* (KB).

MATERIALS AND METHODS

Expanded Materials and Methods are presented in the **supplemental data** (Supplemental Digital Content 1, http://links.lww.com/CCM/C97). GPx1 knockout (−/−) and wild-type (WT) mice on a C57BL/6J background were used (17). Group allocations of mice were random depending on their genotype.

Animal Experiments

Experiments were approved by the Alfred Medical Research and Education Precinct Animal Ethics Committee, Melbourne, VIC, Australia. The mouse model of acute pneumonia has been validated and published previously (18). Equal numbers of male and female mice were used (n = 17 to 20 for survival experiments and 6 to 10 for biochemistry and pathology experiments). Mice were 10–12 weeks old.

Tissue Collection

Klebsiella pneumoniae (5×10^3 colony-formatting units)–infected mice were euthanized on days 1 and 2 post infection. Lungs and plasma were collected. Lungs were processed for immunohistochemical analysis or stored at −80°C for RNA and protein extraction.

Quantitative Real-Time Polymerase Chain Reaction

Adhesion molecules, proinflammatory cytokines, and oxidative stress markers were assessed in lung homogenates as previously described (19).

Lung Tissue and Circulating Inflammatory Markers

IL-6, IL-1β, IL-10, and interferon-γ (IFN-γ) were measured in lung homogenates and plasma by using commercially available enzyme-linked immunosorbent assay (ELISA) kits (R&D systems, Minneapolis, MN) as per manufacturer's instructions.

Western Blots

Caspase-1 and IL-1β protein were measured by Western blots. Anti-mouse IL-1β primary antibody (number, 8689; Cell Signaling Technology, Danvers, MA) or an anti-mouse caspase-1 primary antibody (number, sc-1218R; SantaCruz Biotechnology, Dallas, TX) and α-tubulin (number, 2144; Cell Signaling Technology) were used. ECL Advance Western Blotting detection and quantitation by densitometry revealed protein levels. Data are expressed relative to α-tubulin.

Histology

Formalin-fixed, paraffin-embedded 4-μm-thick lung sections were stained with hematoxylin and eosin and analyzed for inflammatory infiltrate (assigned a score of 0–5) according to Yatmaz et al (20). Six to seven mouse lungs were analyzed per group. A blinded examiner performed the analysis of the histology slides.

Immunohistochemistry

Nitrotyrosine (1:150; Chemicon, Billerica, MA), 4-hydroxynonenal (4-HNE; 1:125; JaICA; Thermo Fisher, Rockford, IL), and myeloperoxidase (1:100; Thermo Fisher) were detected in lung paraffin sections. Three images were quantitated per mouse, and 8–10 mice were analyzed per group. A blinded examiner performed the analysis of the immunohistochemistry slides.

Bone Marrow Cell Isolation and Bone Marrow–Derived Macrophage Culture

Bone marrow–derived macrophages (BMDMs) were isolated and cultured as previously described (21).

Copyright © 2016 by the Society of Critical Care Medicine and Wolters Kluwer Health, Inc. All Rights Reserved.

Stimulation of BMDMs

BMDMs were primed for 12 hours with lipopolysaccharide (LPS) (1 μg/mL) and then infected with KB as previously described (22).

ROS Detection

After BMDM infection, DMEM containing fluorescent probes (peroxyfluor-6 acetoxylmethyl at 5 μM or dihydroethidium at 5 μM) replaced DMEM containing bacteria. A multimode microplate reader (FLUOstar, BMG labtech, Ortenberg, Germany) captured fluorescence. Two experiments were analyzed with $n = 6$ per treatment group.

Antioxidant Treatment and Inhibition of ROS Production

To study the role of ROS in NLRP3 activation, three molecules involved in H_2O_2 reduction were used (1): *N*-acetylcysteine (NAC) (0.1 mM) (22) (Sigma-Aldrich, St. Louis, MO) (2), catalase (1 IU/μl) (Sigma-Aldrich), and (3) 2-phenly-1,2-benzisoselenazol-3[2*H*]-one (ebselen) (0.01 μM). Two global inhibitors of ROS production were the nicotinamide adenine dinucleotide phosphate inhibitor, apocynin (600 μM) (Sigma-Aldrich), and the mitochondria complex I inhibitor, rotenone (20 μM). The MCC950 inhibitor from Cayman (Cayman Chemical, Ann Arbor, MI) was used to inhibit the NLRP3 inflammasome (100 and 1,000 nM). BMDMs were treated with the different molecules for 30 minutes before infection with KB. After 4 hours, the supernatant was harvested for IL-1β and caspase-1 ELISA measurements. Two independent experiments were analyzed with $n = 6$ per treatment group.

Statistical Analysis

Differences in survival were assessed by log-rank analysis and represented by Kaplan-Meier curves. All other experiments were analyzed using one-way analysis of variance with post hoc analysis (Fisher least significant difference test or Bonferroni multiple comparison tests). *p* value less than 0.05 was considered significant. Error bars represent SEM.

RESULTS

GPx1$^{-/-}$ Mice Show Increased Survival With an Increased Transient Activation of the Innate Immune Response During Acute Pneumonia

We observed a significant increase in survival of GPx1$^{-/-}$ mice compared to WT mice: 59.1% versus 29.2% (**Fig. 1*A***). Treatment with redox modulators (NAC or ebselen by intraperitoneal injection) at the same time as bacterial inoculation and twice daily 24 hours after infection significantly decreased survival of GPx1$^{-/-}$ mice over the 5-day monitoring period: GPx1$^{-/-}$ 55% to GPx1$^{-/-}$ + ebselen 17%; GPx1$^{-/-}$ + NAC 30% (**Fig. 1*B***).

We performed hematoxylin and eosin staining on lung sections 1 and 2 days post infection and assessed the severity of infection (23). GPx1$^{-/-}$ mice lungs showed a significant increase in inflammatory infiltrate of leukocytes on day 1 compared with day 1-infected WT lungs ($p < 0.05$) (**Fig. 1*C***). Analysis of myeloperoxidase levels to detect neutrophils showed a significant increase on day 2 in WT lungs that was significantly attenuated on day 2 in GPx1$^{-/-}$ lungs, suggestive of enhanced resolution of infection in GPx1$^{-/-}$ lung tissue at this time point (**Fig. 1*D***).

NLRP3 inflammasome activation was measured by the concentration of inactive and active forms of caspase-1 and IL-1β by Western blot in the lung on days 1 and 2 post infection. GPx1$^{-/-}$ mice lungs showed a significant increase in the p20 active form of caspase-1, as well as the activated 17.5-kD subunit of IL-1β on day 1 after infection. A significant decrease in caspase-1 p20 and IL-1β 17.5-kD subunits was observed on day 2. No significant changes were observed in caspase-1 p20 and IL-1β 17.5-kD subunits in the lungs of WT mice. No significant change was observed in the inactive caspase-1 p45 subunit on either day in both WT and GPx1$^{-/-}$ lungs, with only the inactive IL-1β 35-kD subunit showing a decline on day 2 in GPx1$^{-/-}$ lungs (**Fig. 1**, ***E*** and ***F***).

We measured IL-1β protein levels in the lung and plasma by ELISA. Changes in IL-1β protein exhibited a similar pattern in the lung of GPx1$^{-/-}$ mice compared with Western blot analysis with respect to an early significant increase in IL-1β levels on day 1 and a decline on day 2 when compared with control lungs (**Fig. 1**, ***G*** and ***H***). Expression of IL-1β and NLRP3 genes was transiently but significantly increased on day 1 in GPx1$^{-/-}$ mice, whereas WT mice had significant increases in these genes on day 2 only (**Fig. 1**, ***I*** and ***J***).

To further study the increase in the enhanced innate immune response, we measured IL-6 and IFN-γ concentrations by ELISA in the lungs and plasma on days 1 and 2 after infection. No change was detected in IL-6 concentrations in GPx1$^{-/-}$ mice, whereas a significant increase was observed on day 2 in the lungs and plasma of WT mice (**Fig. 2**, ***A*** and ***B***). A similar pattern was observed for IFN-γ concentration (**Fig. 2**, ***C*** and ***D***). We also measured the concentration of IL-10, a potent anti-inflammatory cytokine, in plasma on days 1 and 2 after infection. IL-10 levels were significantly increased on day 1 and significantly decreased on day 2 in GPx1$^{-/-}$ mice, whereas it was significantly increased on day 2 in WT mice (**Fig. 2*E***).

Lung gene expression of tumor necrosis factor (TNF)-α, IL-6, and IFN-γ, assessed by real-time polymerase chain reaction, showed an early increase in the transcription of TNF-α and IL-6 on day 1 with a significant decrease on day 2 for TNF-α in GPx1$^{-/-}$ mice. On the other hand, transcription was significantly increased on day 2 in WT mice for all three cytokines (**Fig. 2**, ***F–H***).

GPx1$^{-/-}$ Lungs Show an Early Transient Oxidative Stress During Acute Pneumonia

GPx1$^{-/-}$ mice displayed a significant increase in the oxidative stress markers, 4-HNE and nitrotyrosine, in the lung on day 1 with a return to baseline levels on day 2 after infection. No significant changes were observed in lungs from C57Bl/6J mice (**Fig. 3**, ***A*** and ***B***). Transcription of enzymes specifically involved in the reduction of H_2O_2, such as catalase, and the glutathione system, such as glutaredoxin-1 (Grx1) and thioredoxin-1 (Trx1), showed a significant increase on day 1 with a significant

Copyright © 2016 by the Society of Critical Care Medicine and Wolters Kluwer Health, Inc. All Rights Reserved.

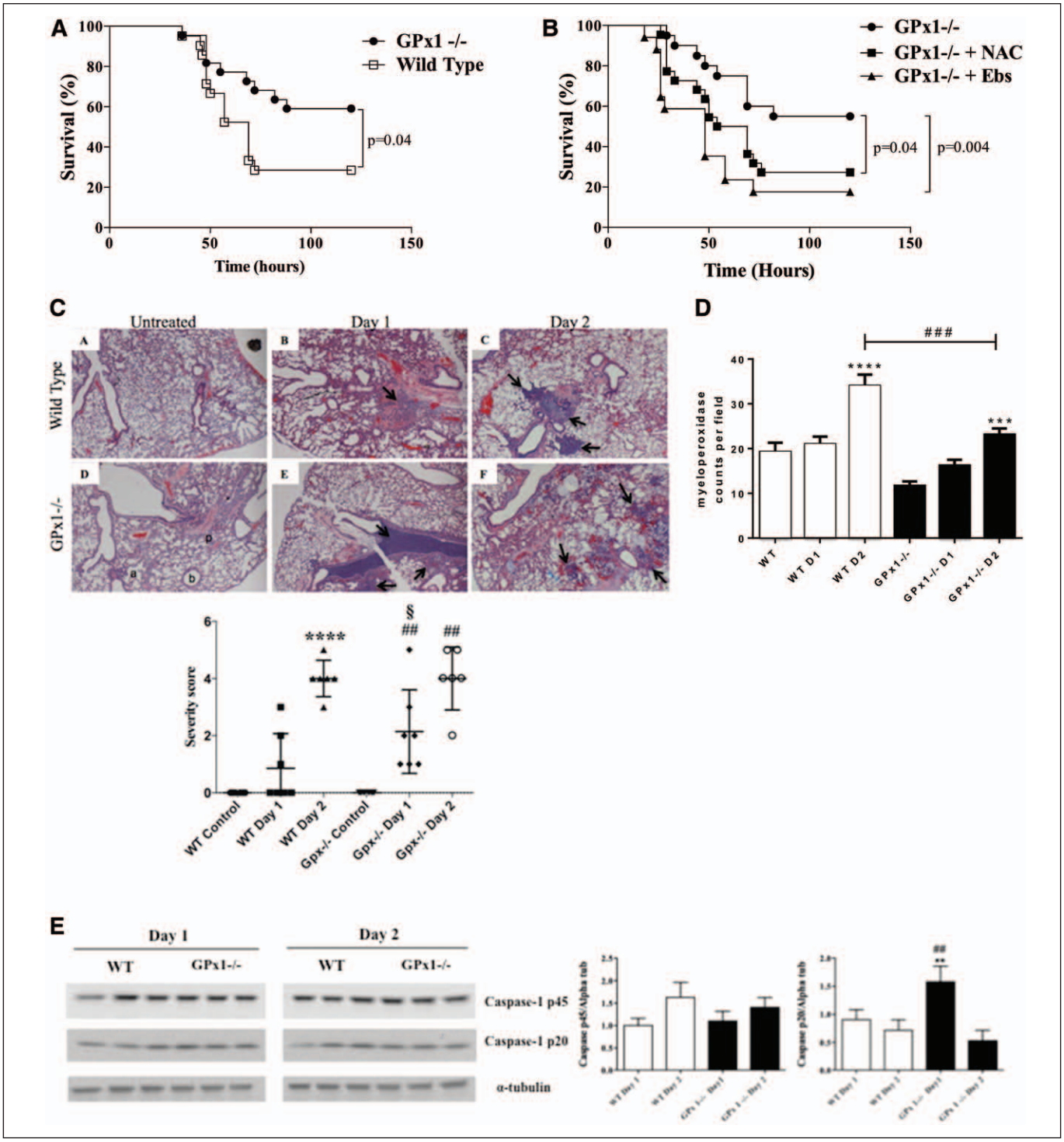

Figure 1. Glutathione peroxidase 1 ($GPx1^{-/-}$) mice show increased survival with an increased transient activation of the innate immune response during acute pneumonia when compared with C57BL/6J mice. **A**, Survival of wild-type (WT) mice ($n = 21$) and $GPx1^{-/-}$ mice ($n = 21$) after intratracheal administration of *Klebsiella pneumoniae* (log-rank test, $p = 0.04$). **B**, Survival of $GPx1^{-/-}$ mice ($n = 20$) and $GPx1^{-/-}$ mice–treated with *N*-acetylcysteine ($n = 20$) or ebselen (Ebs; $n = 17$) after intratracheal administration of *Klebsiella pneumoniae* (log-rank test: $GPx1^{-/-}$ to $GPx1^{-/-}$ + *N*-acetylcysteine [NAC], $p = 0.04$; $GPx1^{-/-}$ to $GPx1^{-/-}$ + Ebs; $p = 0.004$). **C**, Histological analysis of *Klebsiella pneumoniae*–infected WT and $GPx1^{-/-}$ lungs. Hematoxylin and eosin–stained paraffin sections from $GPx1^{-/-}$ lungs displayed increased peribronchial and parenchymal inflammation on day 1 (**E**) compared with infected WT mice on day 1 (**B**) as indicated by the *arrows*. **C** and **F**, Leukocyte infiltrate increased on day 2 in both WT and $GPx1^{-/-}$ lungs. Images are representative of the pattern observed in 6–7 animals. Magnification, ×40. Structures are indicated as follows: a = alveolus, *p* = parenchyma, and b = bronchus. **** $p < 0.0001$ to WT control (CTL); ## $p < 0.01$ to $GPx1^{-/-}$ CTL; § $p < 0.05$ to WT day 1. **D**, Immunohistochemical detection of myeloperoxidase in lung sections on day 1 (D1) and day 2 (D2) after infection. **** $p < 0.0001$ vs WT mice; *** $p < 0.001$ vs $GPx1^{-/-}$ mice; ### $p < 0.001$ D2 WT vs $GPx1^{-/-}$ mice. **E**, Representative Western blots of caspase-1 shown on left and quantitation shown on right. Active caspase-1 (p20) is increased on day 1 (## $p < 0.01$ to WT day 1) and decreased on day 2 (** $p < 0.01$ to $GPx1^{-/-}$ day 2) in $GPx1^{-/-}$ mice, whereas no change is observed in WT mice. Analysis of variance (ANOVA), Bonferroni multiple comparison test, $n = 6$ to 7 per group.

Copyright © 2016 by the Society of Critical Care Medicine and Wolters Kluwer Health, Inc. All Rights Reserved.

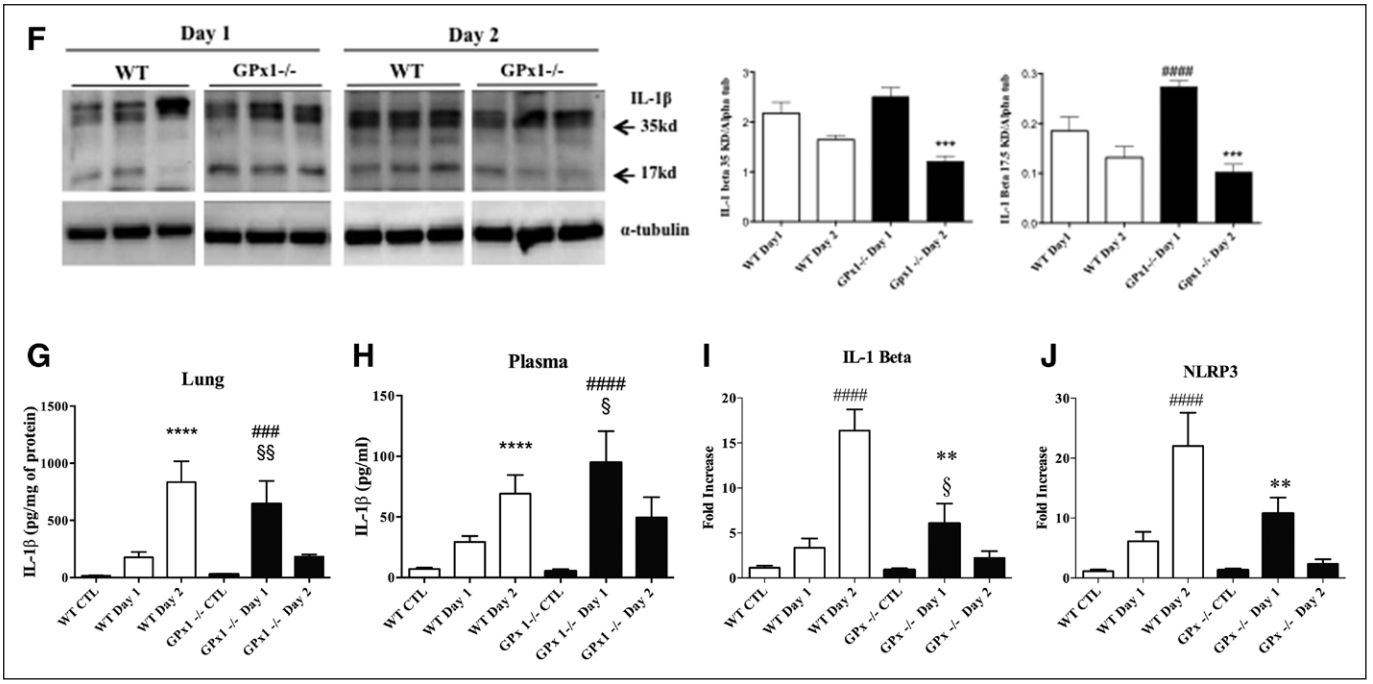

Figure 1. (*Continued*). F, Representative Western blots of interleukin (IL)-1β shown on left and quantitation shown on right. Active IL-1β (17.5-kD subunit) is increased on day 1(####$p < 0.0001$ to WT day 1) and decreased to baseline on day 2 (***$p < 0.001$ to GPx1$^{-/-}$ day 2) in GPx1$^{-/-}$ mice, whereas no change is observed in WT mice. IL-1β precursor (35-kD subunit) decreased on day 2 (***$p < 0.001$ to GPx1$^{-/-}$ day 1) in GPx1$^{-/-}$ lungs after infection. ANOVA, Bonferroni multiple comparison test, $n = 7$ per group. **G**, IL-1β in the lungs, measured by ELISA, was increased on day 1 (###$p < 0.001$ to GPx1$^{-/-}$ CTL) and decreased on day 2 (§§$p < 0.01$ to GPx1$^{-/-}$ day 2). ****$p < 0.0001$ to WT CTL. **H**, IL-1β in plasma, measured by ELISA, was increased on day 1(####$p < 0.0001$ to GPx1$^{-/-}$ CTL) and decreased on day 2 (§$p < 0.05$ to GPx1$^{-/-}$ day 2). ****$p < 0.0001$ to WT CTL. **I**, IL-1β gene expression in lung was increased on day 1 (**$p < 0.01$ to GPx1$^{-/-}$ CTL) and decreased on day 2 (§$p < 0.05$ to GPx1$^{-/-}$ day 2). ####$p < 0.0001$ to WT CTL. **J**, NOD-like receptor family, pyrin domain containing 3 (NLRP3) gene expression in lung was increased on day 1 (**$p < 0.01$ to GPx1$^{-/-}$ CTL) and increased on day 2 in WT mice (####$p < 0.0001$ to WT CTL). **D**–**G**, ANOVA, Fisher least significant difference test, $n = 7$ per group.

decrease on day 2 in GPx1$^{-/-}$ mice, whereas a significant increase was only observed on day 2 in WT mice for catalase and Grx1. A significant increase was observed on day 1 for Trx1 that was maintained on day 2 in control mice (**Fig. 3**, ***C–E***). SOD1 transcription levels were increased in the lungs of GPx1$^{-/-}$ mice on day 2, whereas no changes were observed in WT mice. SOD2 was significantly increased on day 2 in WT mice, whereas no change was observed in the lungs of GPx1$^{-/-}$ mice. Heme oxygenase-1 was significantly increased on day 2 in WT mice, whereas no change was observed in GPx1$^{-/-}$ mice (**Fig. 3**, ***F–H***).

Increase of NLRP3 Inflammasome Activity Is Mediated by H_2O_2 in BMDMs

IL-1β concentrations were significantly increased in GPx1$^{-/-}$ BMDM at multiple of infection (MOI) 10 and MOI 100 compared with uninfected GPx1$^{-/-}$ BMDM, whereas the increase was only significant at MOI 100 for WT macrophages. In addition, the concentration of IL-1β was significantly higher in the GPx1$^{-/-}$ BMDM at MOI 100 compared with WT BMDM infected at MOI 100 (**Fig. 4*A***). Similarly, caspase-1 was significantly increased in GPx1$^{-/-}$ BMDM at MOI 10 and MOI 100 compared with uninfected GPx1$^{-/-}$ BMDM. However, this increase was only significant at MOI 10 for WT macrophages. A small albeit significant increase in caspase-1 was observed in GPx1$^{-/-}$ BMDM at MOI 100 compared with WT BMDM infected at MOI 100 (**Fig. 4*B***).

Infected GPx1$^{-/-}$ BMDMs displayed significantly increased H_2O_2 levels at both 10 and 100 MOI compared with WT BMDM. A smaller although significant increase was observed in WT BMDM at an MOI of 100. In contrast, no significant differences were observed between GPx1$^{-/-}$ and WT BMDMs with respect to $O_2^{\cdot-}$ production (**Fig. 4**, ***C*** and ***D***). Catalase, NAC, and ebselen significantly decreased the concentration of caspase-1 and IL-1β in GPx1$^{-/-}$ BMDMs at MOI 10 and MOI 100. Global inhibition of ROS production with apocynin and rotenone also significantly decreased caspase-1 and IL-1β concentrations (**Fig. 4**, ***E*** and ***F***). To demonstrate a role for H_2O_2 in the activation of the inflammasome, we infected LPS-treated WT BMDMs with MOI 10 and MOI 100 KP bacteria and exposed them to two concentrations of H_2O_2. Caspase-1 levels were significantly increased by both concentrations of H_2O_2 (**Fig. 4*G***). Finally, to show the involvement of the NLRP3 inflammasome in the activation of caspase-1 in our system, we used the NLRP3 inhibitor, MCC950, in the presence of LPS-primed BMDMs, MOI 100 bacteria, and two doses of the inhibitor. Both inhibitor concentrations significantly lessened caspase-1 levels (**Fig. 4**, ***H*** and ***I***).

IL-1 Receptor Antagonist Anakinra Abolishes the Resistance Against Acute Pneumonia in GPx1$^{-/-}$ Mice

Survival was significantly decreased in GPx1$^{-/-}$ mice–treated with anakinra (IL-1 receptor antagonist): GPx1$^{-/-}$ mice = 57.1% versus

Copyright © 2016 by the Society of Critical Care Medicine and Wolters Kluwer Health, Inc. All Rights Reserved.

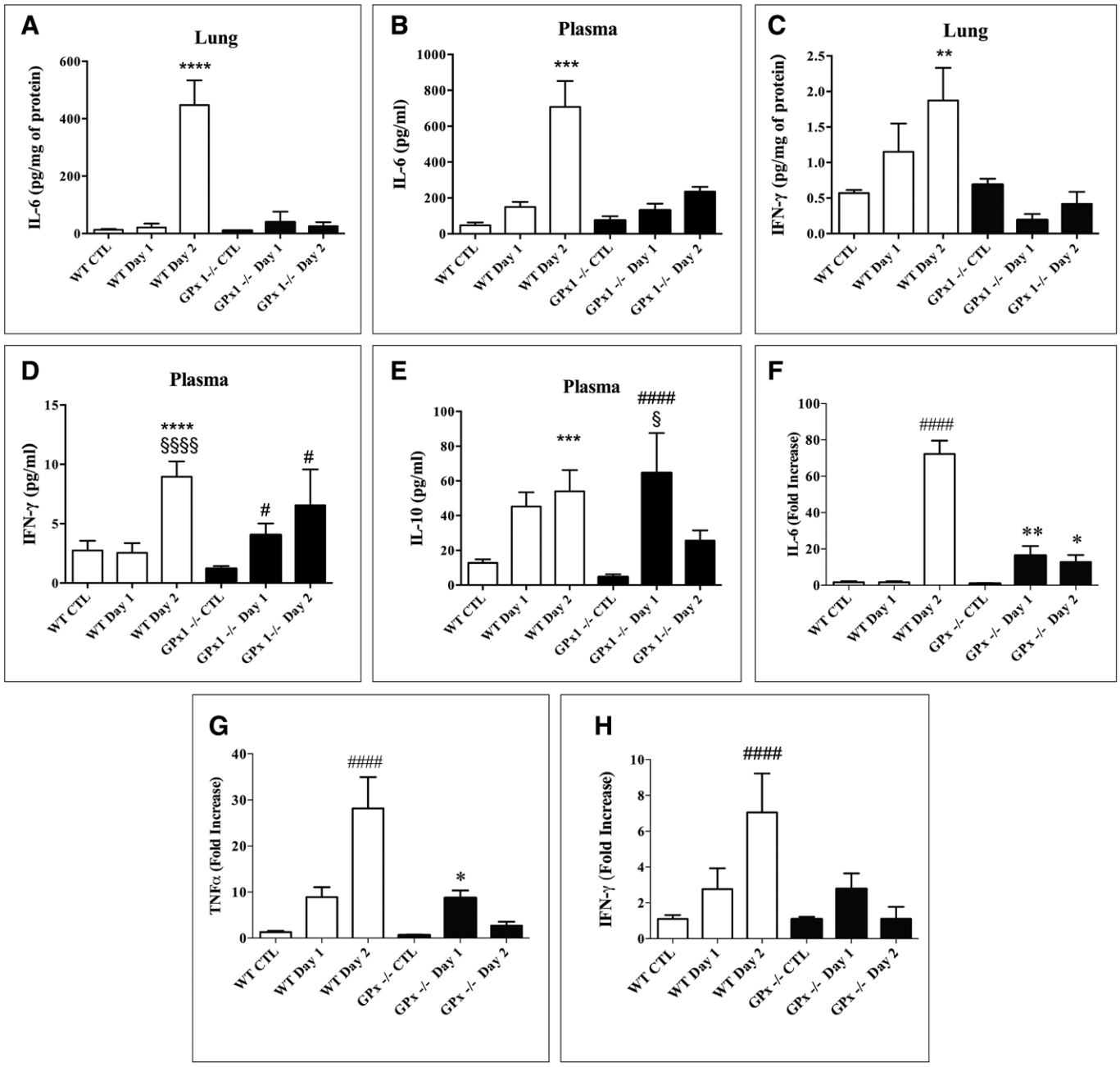

Figure 2. Lung and systemic inflammatory responses are significantly increased in wild-type (WT) mice compared with glutathione peroxidase 1 (*GPx1*$^{-/-}$) mice. **A**, Lung interleukin (IL)-6 protein levels: ****$p < 0.0001$ to WT control (CTL). $n = 7$ per group. **B**, Plasma IL-6 protein levels: ***$p < 0.001$ to WT CTL. $n = 10$ per group. **C**, Lung interferon (IFN)-γ protein levels: **$p < 0.01$ to WT CTL. $n = 7$ per group. **D**, Plasma IFN-γ protein levels: ****$p < 0.0001$ to WT CTL; §§§§$p < 0.0001$ to WT day 1. In GPx1$^{-/-}$ plasma, #$p < 0.05$ to GPx1$^{-/-}$ CTL. $n = 10$ per group. **E**, Plasma IL-10 protein levels: ***$p < 0.001$ to WT CTL. In GPx1$^{-/-}$ plasma, ####$p < 0.0001$ to GPx1$^{-/-}$ CTL and §$p < 0.05$ to GPx1$^{-/-}$ day 2. $n = 10$ per group. **F**, Lung IL-6 gene expression: ####$p < 0.0001$ to WT CTL. In GPx1$^{-/-}$ lung, *$p < 0.05$ and **$p < 0.01$ to GPx1$^{-/-}$ CTL. $n = 7$ per group. **G**, Lung tumor necrosis factor (TNF) gene expression: ####$p < 0.0001$ to WT CTL. In GPx1$^{-/-}$ lungs, *$p < 0.05$ to GPx1$^{-/-}$ CTL. $n = 7$ per group. **H**, Lung IFN-γ gene expression: ####$p < 0.0001$ to WT CTL. $n = 7$ per group. **A**–**H**, Analysis of variance and Fisher least significant difference test.

GPx1$^{-/-}$ + IL-1 RA = 27.7% (**Fig. 5**), strongly suggestive that the resistance to acute pneumonia observed in GPx1$^{-/-}$ mice is facilitated by an increase in the activation of the NLRP3 inflammasome.

DISCUSSION

For decades, research has focused on blunting the innate immune response during septic shock arising from severe infection. This approach has not been successful, and recent clinical evidence suggests that early proinflammatory responses are needed for protection against advancement of septic shock syndrome (8, 9). ROS are regarded as an integral component of septic shock and are considered toxic and harmful when produced as a component of acute inflammatory states. However, this study has shown that early oxidative stress, contrary to expectation, provided protection against septic shock. In mice

Copyright © 2016 by the Society of Critical Care Medicine and Wolters Kluwer Health, Inc. All Rights Reserved.

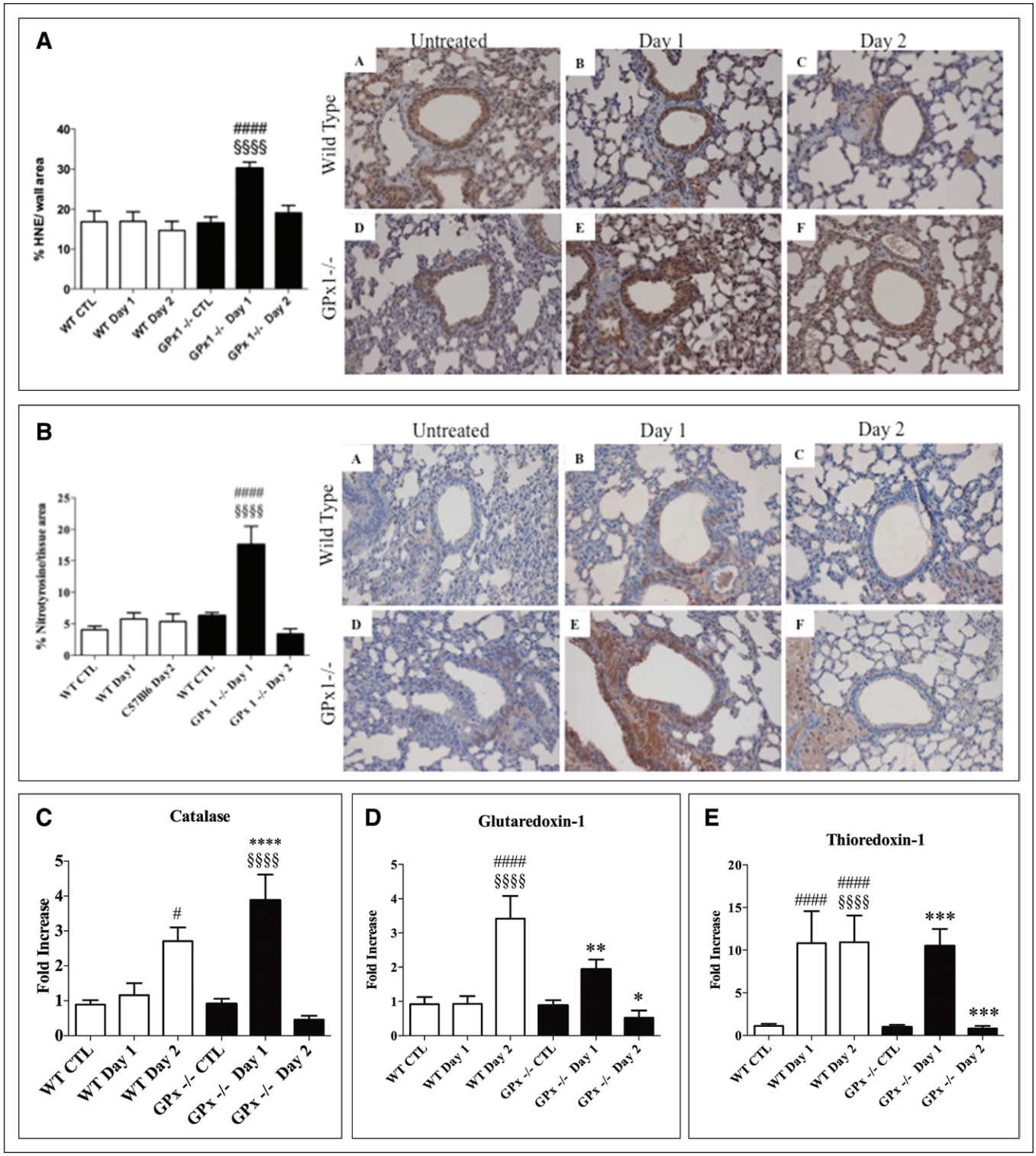

Figure 3. Glutathione peroxidase 1 (*GPx1*$^{-/-}$) lungs show an early transient oxidative stress during acute pneumonia. **A**, 4-Hydroxynonenal (4-HNE) levels (E–B) as indicated by the brown staining. Quantitation is shown on the left. ####$p < 0.0001$ to wild-type (WT) day 1. §§§§$p < 0.0001$ to GPx1$^{-/-}$ day 2. **B**, Nitrotyrosine levels (E–B) as indicated by the brown staining. Quantitation is shown on the left. ####$p < 0.0001$ to WT day 1. §§§§$p < 0.0001$ to GPx1$^{-/-}$ day 2. **C**, Catalase gene expression: ****$p < 0.0001$ to WT day 1 and §§§§$p < 0.0001$ to GPx1$^{-/-}$ day 2. #$p < 0.05$ to WT control (CTL). **D**, GRx1 gene expression: **$p < 0.01$ to WT day 1 and *$p < 0.05$ to GPx1$^{-/-}$ day 1. It increased significantly on day 2 in the WT mice. ####$p < 0.0001$ to WT CTL and §§§§$p < 0.0001$ to WT day 1. **E**, TRx1 gene expression: ***$p < 0.001$ to GPx1$^{-/-}$ CTL and ***$p < 0.001$ to GPx1$^{-/-}$ day 1. A significant and prolonged increase was observed on WT days 1 and 2 after infection, ####$p < 0.0001$ to WT CTL and §§§§$p < 0.0001$ to WT CTL.

Copyright © 2016 by the Society of Critical Care Medicine and Wolters Kluwer Health, Inc. All Rights Reserved.

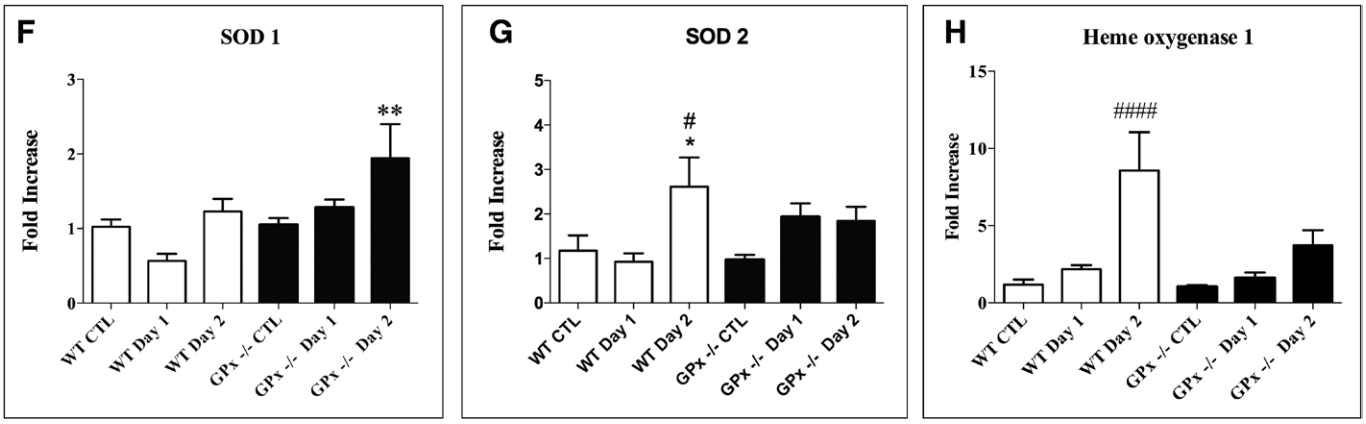

Figure 3. (*Continued*). **F**, Superoxide dismutase (SOD)1 gene expression: $^{**}p < 0.01$ to GPx1$^{-/-}$ CTL. **G** and **H**, SOD2 and heme oxygenase-1 (Hgene expression: SOD1: $\#p < 0.05$ to WT CTL; HMO-1: $\#\#\#\#p < 0.0001$ to WT CTL. **C**–**H**, Analysis of variance, Bonferroni multiple comparison test. $n = 7$–10 per group.

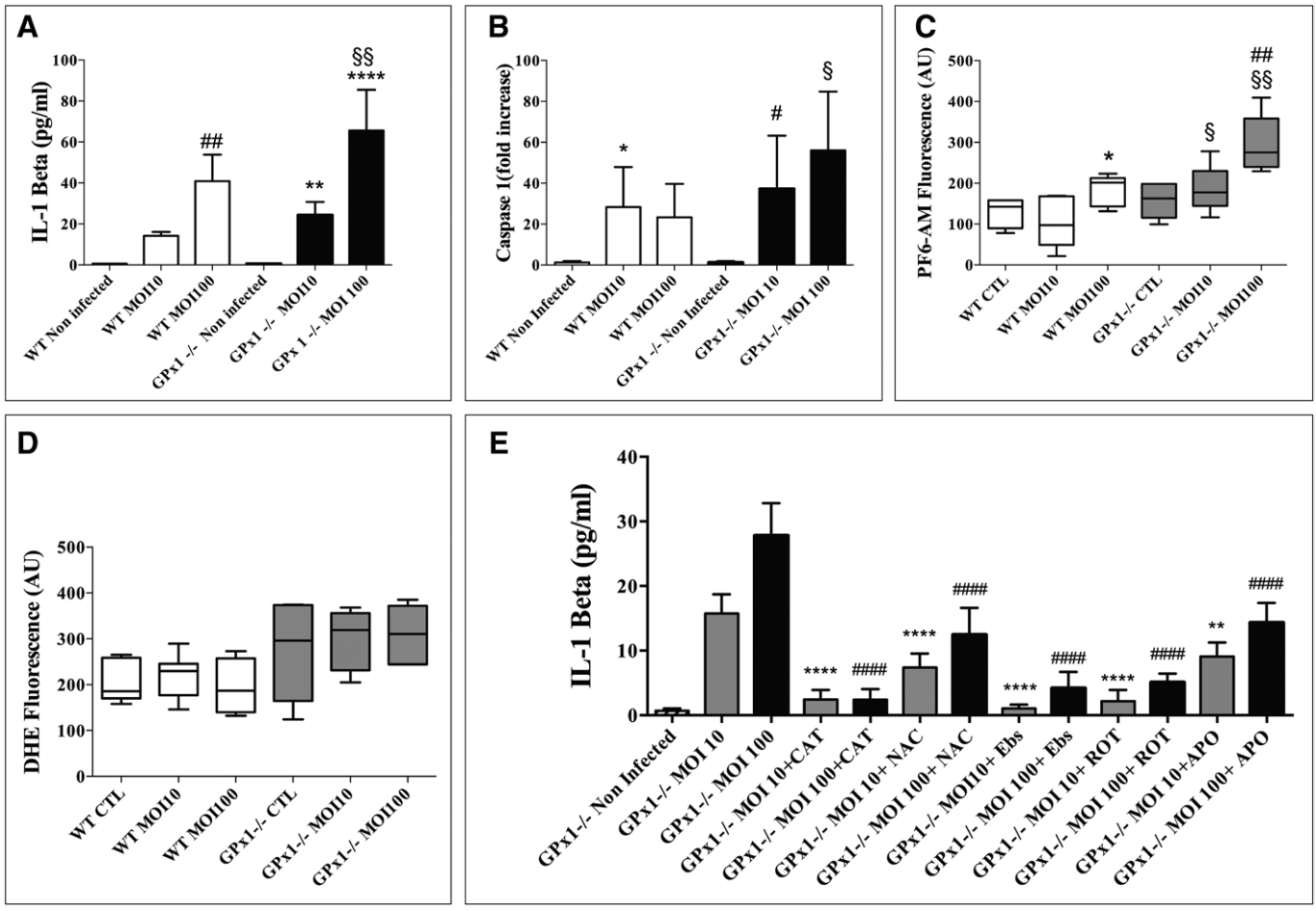

Figure 4. NOD-like receptor family, pyrin domain containing 3 (NLRP3) inflammasome activation is greater in infected glutathione peroxidase 1 (GPx1$^{-/-}$) bone marrow–derived macrophages (BMDMs) than in wild-type (WT) mice and is mediated by a transient increase in H_2O_2 concentration. **A**, In GPx1$^{-/-}$ BMDM, interleukin (IL)-1β in the supernatant was increased at multiple of infection (MOI) 10 ($^{**}p < 0.01$) and 100 ($^{****}p < 0.0001$) versus noninfected GPx1$^{-/-}$ BMDM. §§$p < 0.01$ to WT MOI 100. In WT, IL-1β was increased at MOI 100. ##$p < 0.001$ to WT noninfected BMDM ($n = 6$ per group). **B**, In GPx1$^{-/-}$ BMDM, caspase-1 in the supernatant was higher at MOI 10 ($\#p < 0.05$) and MOI 100 (§$p < 0.05$) versus GPx1$^{-/-}$ noninfected and §$p < 0.05$ to WT MOI 100. In WT, $^{*}p < 0.05$ to WT noninfected BMDM. $n = 6$ per group. **C**, In GPx1$^{-/-}$ BMDM, H_2O_2 assessed by PF6-AM fluorescence was increased at MOI 10 (§$p < 0.05$) and MOI 100 (§§$p < 0.001$) versus WT counterparts. ##$p < 0.01$ to GPx1$^{-/-}$ CTL and MOI 10. In WT, $^{*}p < 0.05$ to WT noninfected BMDM. $n = 6$ per group. **D**, Superoxide anion was unchanged for GPx1$^{-/-}$ and WT BMDM as assessed by dihydroethidium (DHE) fluorescence. $n = 6$ per group. **E** and **F**, Supplementation of GPx1$^{-/-}$ BMDM with antioxidants targeting H_2O_2 (catalase [CAT], NAC, and ebselen [Ebs] decreased IL-1β (**E**) and caspase-1 (**F**) in the supernatant: $^{****}p < 0.0001$ to GPx1$^{-/-}$ MOI 10; $\#\#\#\#p < 0.0001$ to GPx1$^{-/-}$ MOI 100. Inhibitors of ROS production (Apocynin [APO], Rotenone [ROT]) decreased IL-1β (**E**) and caspase-1

Copyright © 2016 by the Society of Critical Care Medicine and Wolters Kluwer Health, Inc. All Rights Reserved.

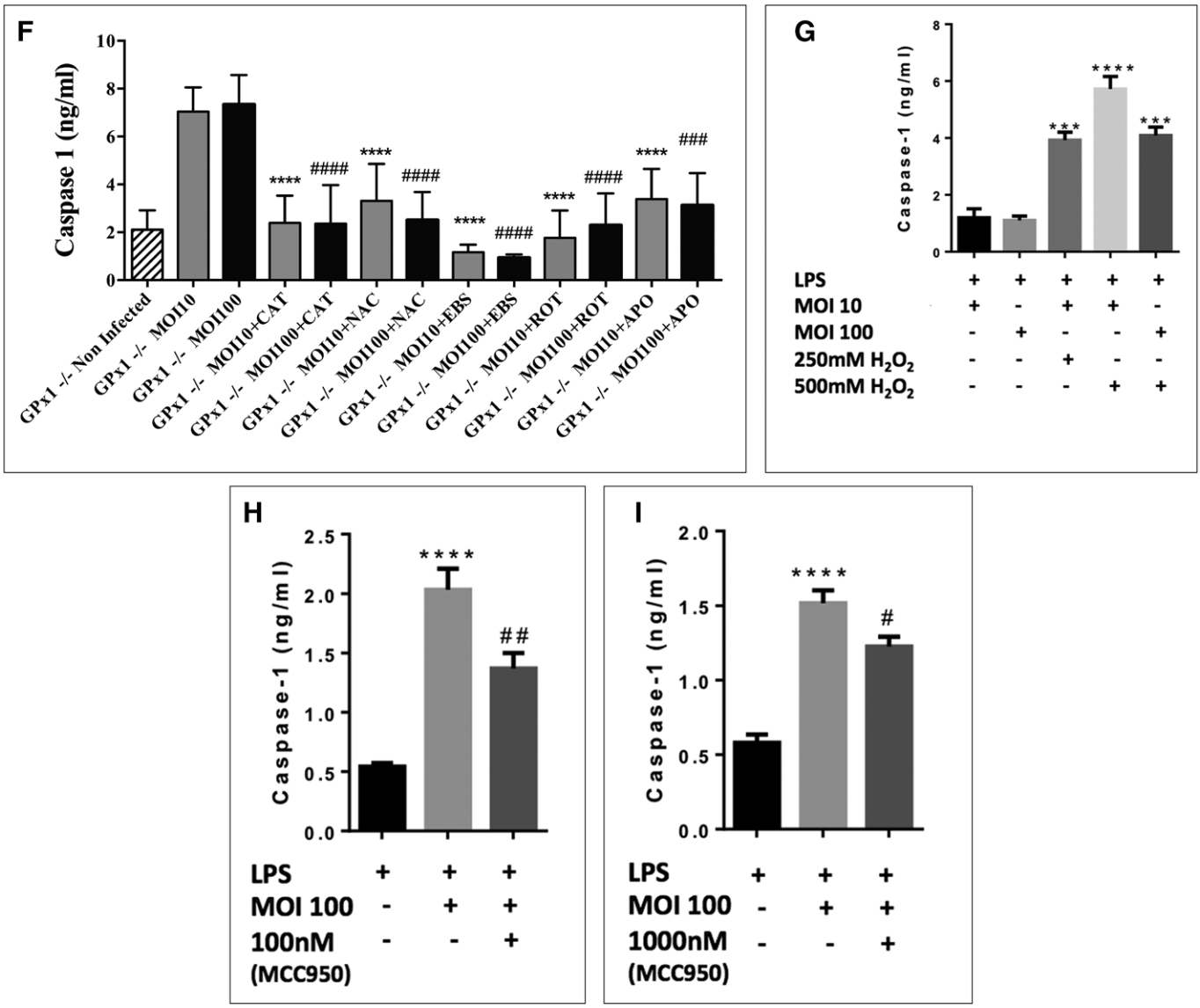

Figure 4. (*Continued*). (F) in the supernatant: $^{**}p < 0.01$; $^{***}p < 0.001$;$^{****}p < 0.0001$ to GPx1$^{-/-}$ MOI 10; ####$p < 0.0001$ to GPx1$^{-/-}$ MOI 100. $n = 6$ per group. **G**, Caspase-1 levels in LPS-primed wild-type BMDM after infection with KP and 250 mM or 500 mM H_2O_2. $^{****}p < 0.0001$; $^{***}p < 0.001$ to LPS and MOI 10 or 100 treated groups. **H** and **I**, Caspase-1 levels in LPS primed wild-type BMDM after infection with KP and two concentration (100 nm [h] and 1,000 nM [i]) of the NLRP3 inhibitor, MCC950. **a-i**, Analysis of variance, Bonferroni multiple comparison test.

deficient for the antioxidant enzyme, GPx1, where ROS levels are increased, we demonstrated a protective effect against sepsis progression during acute pneumonia induced by *Klebsiella pneumonia.* This protective effect was mediated by an early activation of the NLRP3 inflammasome induced by a transient but significant increase in H_2O_2 concentration in the lung.

The activation of the NLRP3 inflammasome is triggered by various environmental prompts, such as extracellular adenosine triphosphate, silica, or pathogen-associated molecular patterns (24–26). These danger signals are known to induce ROS production, and it has been hypothesized that ROS are essential secondary messengers required for NLRP3 inflammasome activation (27). However, the source of ROS in the activation of the NLRP3 inflammasome has been debated (28, 29), and the specific ROS involved have not been fully characterized. Cellular production of ROS regulates several important physiologic responses (30), and as recently emphasized, individual ROS have specific functions based on their chemical properties (31). It has been hypothesized that SOD1 is involved in the activation of NLRP3 based on the results in SOD1 knockout mice (16). An understanding of the ROS mediating its effect in SOD1 knockout mice is less obvious because knockout of SOD1 results in an increase in $O_2^{\cdot-}$ accumulation and a decrease in H_2O_2 production. A recent study has shed light on the potential ROS involved in activation of the inflammasome through indirect means using inhibitors of ROS. Their study identified a role for $O_2^{\cdot-}$ and H_2O_2 in the activation of the inflammasome associated with hyperhomocysteinemia-induced podocyte injury (32). In our model, the knockout of GPx1 specifically increases H_2O_2 accumulation and indeed restoration of H_2O_2 antioxidant defenses abolished the protective effect observed. Furthermore, our in vitro study of bacterially infected macrophages failed to increase superoxide

Copyright © 2016 by the Society of Critical Care Medicine and Wolters Kluwer Health, Inc. All Rights Reserved.

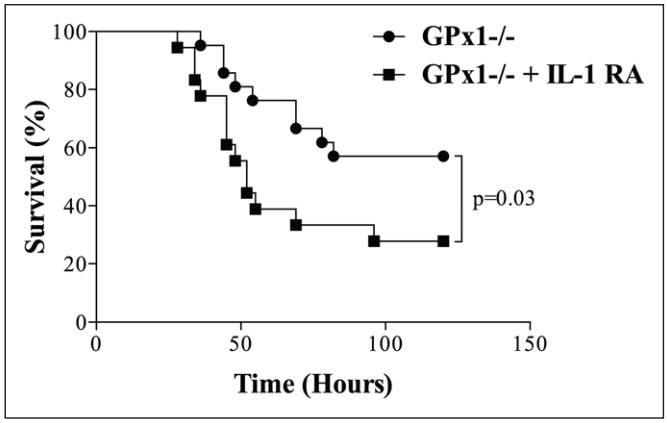

Figure 5. Treatment with IL-1 RA abolishes the protective effect observed during acute pneumonia in glutathione peroxidase 1 ($GPx1^{-/-}$) mice. Intraperitoneal injection of anakinra at 10 mg/kg significantly reduced the survival of $GPx1^{-/-}$ mice during acute pneumonia ($n = 20$ per group). $GPx1^{-/-}$ mice = 57.1% to $GPx1^{-/-}$ + IL-1 RA = 27.7%; log-rank test, $p = 0.03$.

levels but robustly increased H_2O_2 levels, which was associated with increased levels of Il-1β and caspase-1. Therefore, our results strongly imply a role for H_2O_2 in the activation of the NLRP3 inflammasome. These results may be extrapolated to the clinical situation if an intervention like an increase in the fraction of inspired oxygen could lead to a transient increase in H_2O_2. Therefore, more experiments are required to confirm the clinical relevance of these results.

Furthermore, our results suggest the significance of GPx1 in the regulation of H_2O_2-mediated inflammasome activation because the presence of other H_2O_2-degrading enzymes were unable to prevent the activation of the inflammasome in our $GPx1^{-/-}$ mouse model. Several reasons can be postulated to explain the lack of removal of H_2O_2 by other enzymes, such as catalase and peroxiredoxin in the $GPx1^{-/-}$ model, highlighting the superiority of GPx1 in inflammasome activation. Catalase is confined to peroxisomes in most cells where its prime function is to remove H_2O_2 generated by peroxisomal oxidases. It can also remove H_2O_2 produced in other cell compartments but only if it diffuses into these organelles (33). Therefore, the action of catalase is limited. On the other hand, GPx1 is a widely distributed peroxidase enzyme (33, 34), found both in the cytosol and mitochondrion. In the kinetic hierarchy, GPx1 reacts with H_2O_2 almost 10_4 times faster than catalase (35–37). Therefore, it is unlikely that catalase compensates for GPx1 in the removal of H_2O_2 in the GPx1 knockout mouse despite the increased expression observed in the GPx1−/− sepsis model on day 1 after bacterial infection. Peroxiredoxins are localized to cell membranes, particularly those of the mitochondria, where they play an important role in physiologically relevant redox cell signaling (35, 38, 39).

Our findings also highlight that the time course of activation of the innate immune response is critical to avoid growth of the bacterial inoculum. Recent reports have shown that mixed anti-/proinflammatory response profiles or an early anti-inflammatory response may play a key role in the transition from infection to severe sepsis (6, 9). Our results stress the importance of an early but transient proinflammatory response at the initial phase of an infection to avoid the "cytokine storm," leading to the development of severe sepsis. We demonstrate that NLRP3 activation and the release of active IL-1β is an early step in the activation of the innate immune response during acute pneumonia. This transient activation at the site of infection allows earlier leukocyte recruitment and avoids the systemic increase in cytokines, such as IL-6, TNF-α, or IL-10. In addition, our findings agree with clinical studies of community-acquired pneumonia that demonstrate that a worse outcome is associated with a persistent increase in the inflammatory response after day 2 of infection (9). These conclusions have also been suggested to be relevant to patients with severe sepsis (6). However, the timing of intervention is critical for the treatment of septic shock. To confirm the clinical relevance of our results, more experiments are required with an intervention performed after the induction of the infection.

CONCLUSIONS

In summary, our results have provided *in vivo* and *in vitro* evidence that an increase in H_2O_2 is specifically involved in the activation of the NLRP3 inflammasome. An early and transient increase in H_2O_2 is essential for the activation of innate immunity, avoiding the development of a systemic inflammatory response syndrome. Therefore, our results may hold translational promise in the clinic to limit sepsis if early treatment modalities are developed to bolster the triggering of the inflammasome, thereby eliminating bacterial spread and potentially fatal inflammatory responses.

REFERENCES

1. Vincent JL, Marshall JC, Namendys-Silva SA, et al; ICON Investigators: Assessment of the worldwide burden of critical illness: The intensive care over nations (ICON) audit. *Lancet Respir Med* 2014; 2:380–386
2. Bone RC, Balk RA, Cerra FB, et al: Definitions for sepsis and organ failure and guidelines for the use of innovative therapies in sepsis. The ACCP/SCCM Consensus Conference Committee. American College of Chest Physicians/Society of Critical Care Medicine. *Chest* 1992; 101:1644–1655
3. Galley HF: Oxidative stress and mitochondrial dysfunction in sepsis. *Br J Anaesth* 2011; 107:57–64
4. Marshall JC: Why have clinical trials in sepsis failed? *Trends Mol Med* 2014; 20:195–203
5. Osuchowski MF, Craciun F, Weixelbaumer KM, et al: Sepsis chronically in MARS: Systemic cytokine responses are always mixed regardless of the outcome, magnitude, or phase of sepsis. *J Immunol* 2012; 189:4648–4656
6. Tamayo E, Fernández A, Almansa R, et al: Pro- and anti-inflammatory responses are regulated simultaneously from the first moments of septic shock. *Eur Cytokine Netw* 2011; 22:82–87
7. Boomer JS, To K, Chang KC, et al: Immunosuppression in patients who die of sepsis and multiple organ failure. *JAMA* 2011; 306:2594–2605
8. Zobel K, Martus P, Pletz MW, et al; CAPNETZ Study Group: Interleukin 6, lipopolysaccharide-binding protein and interleukin 10 in the prediction of risk and etiologic patterns in patients with community-acquired pneumonia: Results from the German competence network CAPNETZ. *BMC Pulm Med* 2012; 12:6
9. Kellum JA, Kong L, Fink MP, et al; GenIMS Investigators: Understanding the inflammatory cytokine response in pneumonia and sepsis: Results of the Genetic and Inflammatory Markers of Sepsis (GenIMS) Study. *Arch Intern Med* 2007; 167:1655–1663
10. Shimada K, Crother TR, Karlin J, et al: Caspase-1 dependent IL-1β secretion is critical for host defense in a mouse model of *Chlamydia pneumoniae* lung infection. *PLoS One* 2011; 6:e21477

Copyright © 2016 by the Society of Critical Care Medicine and Wolters Kluwer Health, Inc. All Rights Reserved.

11. Witzenrath M, Pache F, Lorenz D, et al: The NLRP3 inflammasome is differentially activated by pneumolysin variants and contributes to host defense in pneumococcal pneumonia. *J Immunol* 2011; 187:434–440
12. Tschopp J, Schroder K: NLRP3 inflammasome activation: The convergence of multiple signalling pathways on ROS production? *Nat Rev Immunol* 2010; 10:210–215
13. Zhou R, Tardivel A, Thorens B, et al: Thioredoxin-interacting protein links oxidative stress to inflammasome activation. *Nat Immunol* 2010; 11:136–140
14. van Bruggen R, Köker MY, Jansen M, et al: Human NLRP3 inflammasome activation is Nox1-4 independent. *Blood* 2010; 115:5398–5400
15. Bauernfeind F, Bartok E, Rieger A, et al: Cutting edge: Reactive oxygen species inhibitors block priming, but not activation, of the NLRP3 inflammasome. *J Immunol* 2011; 187:613–617
16. Meissner F, Molawi K, Zychlinsky A: Superoxide dismutase 1 regulates caspase-1 and endotoxic shock. *Nat Immunol* 2008; 9:866–872
17. de Haan JB, Bladier C, Griffiths P, et al: Mice with a homozygous null mutation for the most abundant glutathione peroxidase, Gpx1, show increased susceptibility to the oxidative stress-inducing agents paraquat and hydrogen peroxide. *J Biol Chem* 1998; 273:22528–22536
18. Huet O, Ramsey D, Miljavec S, et al: Ensuring animal welfare while meeting scientific aims using a murine pneumonia model of septic shock. *Shock* 2013; 39:488–494
19. Soro-Paavonen A, Watson AM, Li J, et al: Receptor for advanced glycation end products (RAGE) deficiency attenuates the development of atherosclerosis in diabetes. *Diabetes* 2008; 57:2461–2469
20. Yatmaz S, Seow HJ, Gualano RC, et al: Glutathione peroxidase-1 reduces influenza A virus-induced lung inflammation. *Am J Respir Cell Mol Biol* 2013; 48:17–26
21. Brotz P, Monack DM: Measuring inflammasomme activation in response to bacterial infection. *In*: The Inflammasome Methods and Protocols. De Nardo CM, Latz E (Eds). New York, Springer, 2013, pp 65–84
22. Victor VM, De la Fuente M: N-acetylcysteine improves in vitro the function of macrophages from mice with endotoxin-induced oxidative stress. *Free Radic Res* 2002; 36:33–45
23. Vlahos R, Stambas J, Bozinovski S, et al: Inhibition of Nox2 oxidase activity ameliorates influenza A virus-induced lung inflammation. *PLoS Pathog* 2011; 7:e1001271
24. Dostert C, Pétrilli V, Van Bruggen R, et al: Innate immune activation through Nalp3 inflammasome sensing of asbestos and silica. *Science* 2008; 320:674–677
25. Fritz JH, Ferrero RL, Philpott DJ, et al: Nod-like proteins in immunity, inflammation and disease. *Nat Immunol* 2006; 7:1250–1257
26. Martinon F, Pétrilli V, Mayor A, et al: Gout-associated uric acid crystals activate the NALP3 inflammasome. *Nature* 2006; 440:237–241
27. Martinon F: Signaling by ROS drives inflammasome activation. *Eur J Immunol* 2010; 40:616–619
28. Zhou R, Yazdi AS, Menu P, et al: A role for mitochondria in NLRP3 inflammasome activation. *Nature* 2011; 469:221–225
29. Heid ME, Keyel PA, Kamga C, et al: Mitochondrial reactive oxygen species induces NLRP3-dependent lysosomal damage and inflammasome activation. *J Immunol* 2013; 191:5230–5238
30. Dickinson BC, Chang CJ: Chemistry and biology of reactive oxygen species in signaling or stress responses. *Nat Chem Biol* 2011; 7:504–511
31. Murphy MP, Holmgren A, Larsson NG, et al: Unraveling the biological roles of reactive oxygen species. *Cell Metab* 2011; 13:361–366
32. Abais JM, Xia M, Li G, et al: Contribution of endogenously produced reactive oxygen species to the activation of podocyte NLRP3 inflammasomes in hyperhomocysteinemia. *Free Radic Biol Med* 2014; 67:211–220
33. Antunes F, Han D, Cadenas E: Relative contributions of heart mitochondria glutathione peroxidase and catalase to H(2)O(2) detoxification in in vivo conditions. *Free Radic Biol Med* 2002; 33:1260–1267
34. Cohen G, Hochstein P: Glutathione peroxidase: The primary agent for the elimination of hydrogen peroxide in erythrocytes. *Biochemistry* 1963; 2:1420–1428
35. Cox AG, Winterbourn CC, Hampton MB: Mitochondrial peroxiredoxin involvement in antioxidant defence and redox signalling. *Biochem J* 2010; 425:313–325
36. Lubos E, Loscalzo J, Handy DE: Glutathione peroxidase-1 in health and disease: From molecular mechanisms to therapeutic opportunities. *Antioxid Redox Signal* 2011; 15:1957–1997
37. Winterbourn CC: The biological chemistry of hydrogen peroxide. *In*: Methods in Enzymology. Pecoraro VL (Ed). Burlington, Elsevier, 2013, pp 3–25
38. Woo HA, Yim SH, Shin DH, et al: Inactivation of peroxiredoxin I by phosphorylation allows localized H(2)O(2) accumulation for cell signaling. *Cell* 2010; 140:517–528
39. Sobotta MC, Liou W, Stöcker S, et al: Peroxiredoxin-2 and STAT3 form a redox relay for H2O2 signaling. *Nat Chem Biol* 2015; 11:64–70

Copyright © 2016 by the Society of Critical Care Medicine and Wolters Kluwer Health, Inc. All Rights Reserved.